

22 July 1991

TO: F. T. Nicholson

FROM: R. M. Vaughan *RMV*

SUBJECT: Revised Gaspra Encounter B-Plane Statistics For EE-2' OPNAV Schedule

This memo presents the results of the latest orbit determination analysis for the LGA Gaspra encounter. It is intended as an update to the results presented in reference [1]. The primary change for the new analysis is the deletion of one OPNAV picture from the previous data arc of 5 pictures and changes in times for the remaining 4 pictures. Also, a new a priori estimate of the spacecraft state uncertainty based solely on radio data has been provided by Vince Poilmeier for use in the simulations. This reflected the actual data that will be available for navigation based on the EE-2' stations allocations in effect on 6/27/91. Finally, this analysis uses the updated a priori uncertainty for the Gaspra ephemeris parameters reported in reference [2].

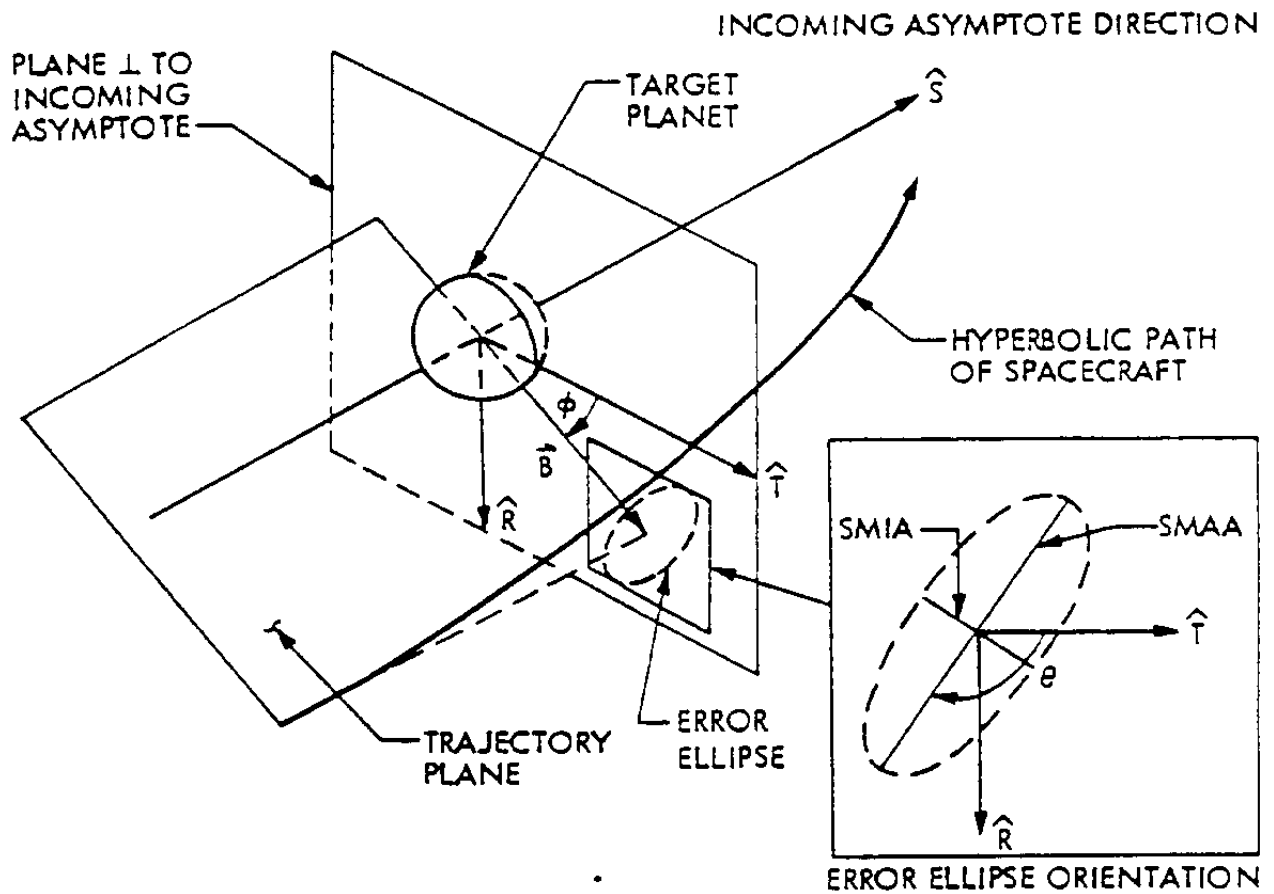
1 A Short Tutorial on B-Plane Statistics

Before presenting the details of the orbit determination simulations, a short discussion of the various methods used to quote B-plane statistics will be given. This is an attempt to clarify some misinterpretations of numbers presented in previous memos.

Figure 1 illustrates the definition of the B-plane and the navigation error ellipse. The spacecraft is assumed to flyby a target body on a hyperbolic trajectory. The B-plane is defined to be normal to the incoming asymptote of the hyperbola or, equivalently, normal to the velocity vector at "infinity" where infinity is defined to be far enough away from the vertex of the hyperbola that the trajectory essentially lies on the asymptote. The directions of the \hat{T} and \hat{R} axes and the \hat{B} vector itself are defined in the figure.

The \hat{B} vector is defined to be the vector from the origin to that point where the asymptote (or V_{∞} vector) intersects the B-plane. For a typical flyby where there is significant bending of the hyperbola due to the gravitational attraction of the target body, the tip of the \hat{B} vector will be farther away from the B-plane origin than the spacecraft at the time it intersects the B-plane. Also, closest approach will generally occur after the spacecraft intersects the B-plane when its position reaches the vertex of the hyperbola. The navigation team internally uses the tip of the \hat{B} vector as its aimpoint. The \hat{B} vector corresponding to a desired closest approach geometry is automatically computed by the navigation software. Usually the coordinates of the \hat{B} vector are of interest only within the navigation team. In the case of the Gaspra flyby where there is almost no gravitational bending of the spacecraft trajectory, the tip of the \hat{B} vector is virtually identical to the spacecraft position at closest approach.

The navigation error ellipse defines the uncertainty associated with hitting the aimpoint in the B-plane. The navigation estimation technique is formulated using Gaussian, or normal, probability distributions. Let the R and T components of \hat{B} be denoted by $B \cdot R$ and $B \cdot T$, respectively. The statistics of these components are assumed to follow the two-dimensional Gaussian distribution with



$$\vec{B} = \text{MISS PARAMETER} = \frac{1}{V_\infty} (\hat{S} \times \vec{H}), \text{ i.e., } \vec{B} \times (V_\infty \hat{S}) = \vec{H}$$

\vec{H} = ANGULAR MOMENTUM VECTOR

V_∞ = VELOCITY AT INFINITY

\hat{T} = PARALLEL TO ECLIPTIC PLANE AND NORMAL TO \hat{S}

$$\hat{R} = \hat{S} \times \hat{T}$$

Figure 1: The Navigation B-plane

probability density function

$$f_{RT} = \frac{1}{2\pi\sigma_R\sigma_T\sqrt{1-\rho_{RT}^2}} \exp \left\{ - \left[\left(\frac{B \cdot R}{\sigma_R} \right)^2 - 2\rho_{RT} \left(\frac{B \cdot R}{\sigma_R} \right) \left(\frac{B \cdot T}{\sigma_T} \right) + \left(\frac{B \cdot T}{\sigma_T} \right)^2 \right] / 2(1-\rho_{RT}^2) \right\}$$

where σ_R and σ_T are the standard deviations for each component and ρ_{RT} is the correlation coefficient between them. The concept of an error ellipse arises naturally when dealing with this type of distribution since contours of constant value of f_{RT} are ellipses. The size and orientation of the B-plane error ellipses are determined by the values of σ_R , σ_T and ρ_{RT} . The standard deviations σ_R and σ_T are the 1σ $B \cdot R$ and $B \cdot T$ values that have been reported in previous memos such as reference [1] discussing navigation performance for the Gaspra encounter. The correlation coefficient ρ_{RT} , which would also be required to reconstruct the error ellipse, has not been reported.

A simple rotation of coordinates can be found for any two dimensional normal distribution such such that the correlation coefficient is zero in the new coordinate system. This is another of the standard ways of reporting navigation B-plane performance. Instead of giving σ_R , σ_T and ρ_{RT} values, the two standard deviations in this special rotated coordinate system are given along with the rotation angle between the original \hat{R} and \hat{T} axes and the new coordinate system. These numbers correspond to the semi-major and semi-minor axes lengths of the error ellipse (SMAA and SMIA in Figure 1) and the rotation angle from the \hat{T} axis to the semi-major axis measured positive clockwise (θ in Figure 1). The standard deviations in $B \cdot R$ and $B \cdot T$ are related to SMAA, SMIA and θ as shown below:

$$\begin{aligned} \sigma_R &= \sqrt{(\text{SMAA} \sin \theta)^2 + (\text{SMIA} \cos \theta)^2} \\ \sigma_T &= \sqrt{(\text{SMAA} \cos \theta)^2 + (\text{SMIA} \sin \theta)^2} \end{aligned}$$

In this memo, 1σ SMAA and SMIA values and the associated θ values will be included along with the 1σ $B \cdot R$ and $B \cdot T$ values.

The probability of the aimpoint being within a certain area in the B-plane is defined to be the integral of the probability density function f_{RT} over that area. Usually this integral is quite difficult to evaluate for an area of arbitrary shape. However, if the area of interest is defined to be an ellipse centered on the nominal aimpoint with semi-major and semi-minor axes lengths of $N\text{SMAA}$ and $N\text{SMIA}$ and an orientation angle θ , integrating f_{RT} gives

$$p(N\sigma) = 1 - e^{-N^2/2}$$

The fact that this integral results in an analytic formula for the probability of being inside an $N\sigma$ error ellipse is related to the fact that the contours of constant value of f_{RT} form ellipses in the B-plane. These are just two of the many special properties of the two-dimensional Gaussian probability distribution. Some probability values computed from the above equation for various values of N are given in the table below:

N	$p(N\sigma)$
1.00	39.35%
2.00	86.47%
2.24	91.86%
3.00	98.89%
4.00	99.97%

Note that these values *are not* the same as the probabilities of being within $N\sigma$ of the nominal value for a one-dimensional Gaussian distribution.

2 OD Simulation Description and Results

The trajectory used for this analysis has Gaspra flyby at 1600 km radial distance, 3.9° N ecliptic latitude on the darkside with closest approach at 22:39:02 UTC on 10/29/91 (DOY 302). This trajectory has nearly constant clock angle during approach as desired for the science observations in EE-3'. The recent change in flyby time to 22:37:00.687 UTC would have no appreciable affect on the results of the OD simulations.

Two optical data arcs were compared in this study. Both had 4 pictures in the period between 53 and 8 days before Gaspra closest approach. For convenience in the subsequent discussion, these two schedules will be referred to as ON1 and ON2. ON1 and ON2 are identical except for the placement of OPNAV #4 which occurs 2 days later for ON2. The ON1 OPNAV picture schedule matches OPNAV commands in the preliminary cruise profile package for EE-2'. SCP 005 has been approved to move OPNAV #4. The ON2 OPNAV picture schedule is to be considered the current baseline schedule. The change should be implemented in the final cruise profile package for EE-2'. The actual times and target stars for these two schedules are shown below:

Picture #	Time of Shutter		Star Content
	SCET (UTC)	Encounter Relative Time	
1	91-249/20:22	-53d 02:17	184489 (magnitude 9.0, spectral class F8) 90141 (magnitude 10.7, spectral class K6)
3	91-271/02:45	-31d 19:54	184459 (magnitude 9.1, spectral class A2)
4 (ON1)	91-284/22:30	-18d 00:09	184459 (magnitude 9.1, spectral class A2)
4 (ON2)	91-286/21:48	-16d 00:51	
5	91-294/14:00	-8d 08:39	184459 (magnitude 9.1, spectral class A2)

Optical data was weighted at 1 pixel for Gaspra images and 0.5 pixel for star images. Gaspra center-finding errors in pixel and line were included as consider parameters with a priori uncertainties of 15% of the image diameter. EME50 camera pointing angles for each picture were estimated as stochastic parameters with a priori uncertainty of 0.1° for RA and DEC. The a priori uncertainty for TWIST was assumed to be 10.0° for OPNAV pictures #1 and 3. Three cases for the a priori uncertainty for TWIST for OPNAV pictures #4 and 5 were investigated. The TWIST uncertainty assumptions for these three cases and the resulting B-plane statistics are presented below.

Case 1 The first case assumed a TWIST uncertainty of 0.25° for both pictures 4 and 5. This is considered the baseline case and represents the best performance that can be expected if all OPNAV pictures are successfully returned and processed. This TWIST uncertainty assumes successful use of the single-frame mosaic technique to image multiple dim stars around Gaspra at the times of the last two OPNAV observations.

Table 1 shows the nominal (1σ) B-plane statistics after incorporation of each OPNAV picture for case 1 for OPNAV pictures schedules ON1 and ON2. The table also lists the a priori B-plane statistics from the radio data solution.

Case 2 The second case assumed a TWIST uncertainty of 10.0° for picture 4 and 0.25° for picture 5. This represents the case where dim stars cannot be seen in picture 4. Picture 4 is more vulnerable to loss of the dim star images required to measure TWIST since it will occur in the scan platform polar region. It should be possible to get the dim star images in picture 5 since a turn will be done to place the observation in the scan platform equatorial region.

Picture Time	1σ B-Plane Errors					Time-of-Flight (sec)
	$B \cdot R$ (km)	$B \cdot T$ (km)	SMAA (km)	SMIA (km)	θ ($^\circ$)	
Radio Only	172.7	117.8	172.7	117.8	90.1	18.5
G-53 ^d	167.3	113.0	167.3	113.1	89.1	18.2
G-31 ^d	159.5	106.0	160.2	105.0	96.8	17.5
ON1 OPNAV Picture Schedule						
G-13 ^d	113.5	91.1	113.5	91.2	91.0	16.3
G-8 ^d	70.8	60.9	75.2	55.4	60.1	14.2
ON2 OPNAV Picture Schedule						
G-16 ^d	107.4	87.5	107.5	87.4	85.3	16.0
G-8 ^d	69.5	60.0	74.0	54.3	59.6	14.1

Table 1: Gaspra B-plane Statistics for Case 1

Table 2 shows the nominal (1σ) B-plane statistics after incorporation of OPNAV pictures 4 and 5 for case 2 for OPNAV picture schedules ON1 and ON2. The statistics prior to incorporation of OPNAV 4 are unchanged from case 1 since the new assumptions for case 2 applied only to the last two pictures. The B-plane statistics in Table 1 for $G - 53d$ and $G - 31d$ are the same for case 2.

Picture Time	1σ B-Plane Errors					Time-of-Flight (sec)
	$B \cdot R$ (km)	$B \cdot T$ (km)	SMAA (km)	SMIA (km)	θ ($^\circ$)	
ON1 OPNAV Picture Schedule						
G-18 ^d	114.4	102.8	115.3	101.8	74.8	17.3
G-8 ^d	72.0	64.7	78.6	56.5	54.8	14.4
ON2 OPNAV Picture Schedule						
G-16 ^d	112.2	99.9	116.6	94.8	62.3	17.1
G-8 ^d	71.8	64.3	79.0	55.1	54.3	14.4

Table 2: Gaspra B-plane Statistics for Case 2

Case 3 The third case assumed a TWIST uncertainty of 10.0° for both pictures 4 and 5. This is included as a worst case scenario in which dim stars are not visible in any of the OPNAV pictures. It does, however, assume that all 4 pictures are successfully returned and processed.

Table 3 shows the nominal (1σ) B-plane statistics after incorporation of OPNAV picture 5 for case 3. The statistics prior to incorporation of OPNAV 4 are unchanged from case 1 since the new assumptions for case 3 applied only to the last two pictures. The B-plane statistics in Table 1 for $G - 53d$ and $G - 31d$ are the same for case 3. Furthermore, the statistics after incorporation of OPNAV 4 for this case are identical to those given for $G - 13d$ and $G - 16d$ in Table 2 for case 2 since the TWIST uncertainty was changed for OPNAV picture 5 only.

Picture Time	1σ B-Plane Errors					Time-of-Flight (sec)
	$B \cdot R$ (km)	$B \cdot T$ (km)	SMAA (km)	SMIA (km)	θ ($^\circ$)	
ON1 OPNAV Picture Schedule						
G-8 ^d	94.5	83.3	112.5	56.7	51.0	15.9
ON2 OPNAV Picture Schedule						
G-8 ^d	95.9	84.4	115.2	55.3	50.9	16.0

Table 3: Gaspra B-plane Statistics for Case 3

References

- [1] Vaughan, R. M., "Gaspra Encounter B-plane Statistics for LGA EE-2' OPNAV Schedule." JPL IOM GLL-NAV-91-96, June 17, 1991.
- [2] Yeomans, D. K., "Updated Uncertainty Analysis for Asteroid 951 Gaspra." JPL IOM 314.6-1289, June 21, 1991.

Distribution

S. P. Synnott	301-125L	K. E. Savary	264-419	K. L. Buxbaum	264-765
R. P. Davis	264-211	R. J. Reichert	264-419	D. A. Bliss	264-765
J. E. Riedel	301-125L	J. A. Dunne	264-765	P. J. Schulte	264-765
W. E. Kirhofer	264-211	R. Gershman	264-765	K. P. Klaasen	168-222
V. M. Pollmeier	261-211	J. M. Ludwinski	264-765	A. P. Harch	264-765
P. H. Kallemeyn	264-211	E. E. Theilig	264-765	H. Breneman	264-765
R. J. Haw	264-211	J. M. Kehrbaum	264-765	B. Roman	264-765
L. A. D'Amario	264-201	B. A. McLaughlin	264-765	R. Phillips	264-765
E. H. Maize	264-211			L. K. Tampari	264-765
				C. Byrne	264-765